Brazilian Journal of Physics (2023) 53:90
https://doi.org/10.1007/s13538-023-01304-x

NUCLEAR PHYSICS

Determination of Photonuclear Reaction Cross-Sections on Stable P-shell Nuclei by Using Deep Neural Networks

Serkan Akkoyun[1,3] · Hüseyin Kaya[1] · Abdulkadir Şeker[2,3] · Saliha Yeşilyurt[2,3]

Received: 30 January 2023 / Accepted: 18 April 2023

Abstract
Photonuclear reactions are widely used in investigations of nuclear structure. Thus, the determination of the cross-sections are essential for the experimental studies. In the present work, (γ, n) photonuclear reaction cross-sections for stable p-shell nuclei have been estimated by using the neural network method. The main purpose of this study is to find neural network structures that give the best estimations for the cross-sections, and to compare them with the available data. These comparisons indicate the deep neural network structures that are convenient for this task. Through this procedure, we have found that the shallow NN models, tanh activation function is better than the ReLU. However, as our models become deeper, the difference between tanh and ReLU decreases considerably. In this context, we think that the crucial hyperparameters are the size of the hidden layer and neuron numbers of each layer.

Keywords Photonuclear reaction · Cross-section · p-shell nuclei · Neural network

1 Introduction

In nuclear structure studies, reactions induced by photons are one of the important tools. In these types of nuclear reaction, the target nuclei are bombarded by high-energy photons, which can statistically be absorbed by a nucleus in the target material. These processes are called photonuclear reactions [1]. Then, the excited nucleus emits a proton, a neutron, an alpha and light particles to get rid of the excitation energy. In the case of neutron emission, the reaction is called as a photo-neutron (γ, n) reaction. Due to the fact that photon is associated with purely electromagnetic interaction with the nuclei, the process is non-destructive. Therefore, it can be used for understanding nucleon-nucleon interaction, collective motion of the nuclear matter and nuclear excitation mechanisms. In the 15-30 MeV energy region, photonuclear reaction cross-sections are large, and stable nuclei may be transmuted to short-lived or stable ones. Although the experimental studies of these reactions have begun in 1934 [2], there is still a lack of existing data. Therefore, systematic studies of photonuclear reactions on different nuclei are needed [3].

The cross-section of photo-neutron reactions for different isotopes at different energies are determined experimentally or by theoretical methods [4, 5]. One of the most used theoretical computer codes for this purpose is the TALYS. The TENDL-2019 database [6] is based on this code and other sources such as ENDF. The code is a system for the analysis and prediction of nuclear reactions. The basic objective behind its construction is the simulation of nuclear reactions that involve neutrons, photons, protons, deuterons, tritons, ^{3}He- and alpha-particles, in the 1 keV-200 MeV energy range and for target nuclides of mass 12 and heavier. To achieve this, it is implemented a suite of nuclear reaction models into a single code.

One of the easiest ways to produce radioactive isotopes is a photo-neutron (γ, n) reaction. ^{8}Be, ^{9}B, ^{11}C, ^{13}Ne and ^{15}O can be generated by using photo-neutron reactions on ^{9}Be, ^{10}B, ^{12}C, ^{14}Ne and ^{16}O stable isotopes. Therefore, the information about the cross-sections of these reactions on p-shell nuclei at different energies is very important. In the literature, there is no complete data for all photon energies on the isotopes

✉ Serkan Akkoyun
sakkoyun@cumhuriyet.edu.tr

1 Department of Physics, Faculty of Science, Sivas Cumhuriyet University, Sivas, Turkey

2 Department of Computer Engineering, Faculty of Engineering, Sivas Cumhuriyet University, Sivas, Turkey

3 Artificial Intelligence Systems and Data Science Application and Research Center, Sivas Cumhuriyet University, Sivas 58140, Turkey

Published online: 13 May 2023

[7]. In the present study, neural network methods have been employed to predict (γ, n) reaction cross-sections on stable or long-lived p-shell nucleus, at energies ranging from the reaction threshold to 200 MeV. The available cross-section data are taken from the TENDL library. The methods generate their own outputs as close as the desired values. One of the advantages of the method is that it does not need any relationship between input and output data variables. Another advantage is that, in the case of missing data, it can complete it by means of its learning ability. Therefore, one can confidently estimate the cross-sections for the given target and energy values that are not available in the literature.

While performing machine learning, we wanted to keep the number of machine learning data higher by using the TENDL data obtained from the theoretical model result, instead of using the limited experimental data available in the literature. The fact that there are about 50 data on the reaction cross sections of the nuclei (γ, n) in this shell means that a good training cannot be made for the nuclei in the p-shell. For this purpose, we wanted to teach the behaviour of the cross-section in this region to the machine by training with a larger data set of theoretical model results. However, by comparing the outputs obtained as a result of machine learning with the available experimental data [7], we investigated whether an improvement could be achieved on the theoretical model results. Recently, neural networks have been used in many fields in nuclear physics. Among them, the studies performed by our group are developing nuclear mass systematic [8], obtaining fission barrier heights [9], obtaining nuclear charge radii [10], estimation of beta decay energies [11], an approximation to the cross-sections of Z boson [12, 13], determination of gamma-ray angular distributions [14], adjustment of relativistic mean-field model parameters [15], neutron-gamma discriminations [16, 17] and estimations of radiation yields for electrons in absorbers [18].

2 Material and Methods

NN (neural network) methods are very powerful mathematical toolsfor almost all problems which are based on the brain functionality and nervous system [19]. They are composed of layers classified in three main groups as input, hidden and output. In each layer,there are artificial neuron cells for the aim of processing the data. Because of the layered structure, a particular type of NN is called layered NN. In the layered feed-forward NN, the neurons in a layer are connected to the neurons only in the next layer by adaptive synaptic weights and data flows forward direction. The input neurons receive the input datawhich are independent variables of the problem. Then the received data is transmitted to the hidden layer neurons by multiplying the corresponding weight values of the connections. All data entering the hidden neurons are summed by using a chosen summation function for obtaining the net valueinside the neuron. After, the net data are activated by an appropriate activation function. The hidden neuron activation function can be theoretically any well-behaved nonlinear function. In this study, tanh (tangent hyperbolic) or ReLU (rectified linear unit) functions have been used for the activations. The advantage of ReLU is its unsaturated gradient, which greatly speeds up the convergence of stochastic gradient landing compared to tanh functions. In the last hidden layer, the data is transmitted to the output layer neurons and NN outputs have been obtained for the dependent variables of the problem. In Fig. 1, we have

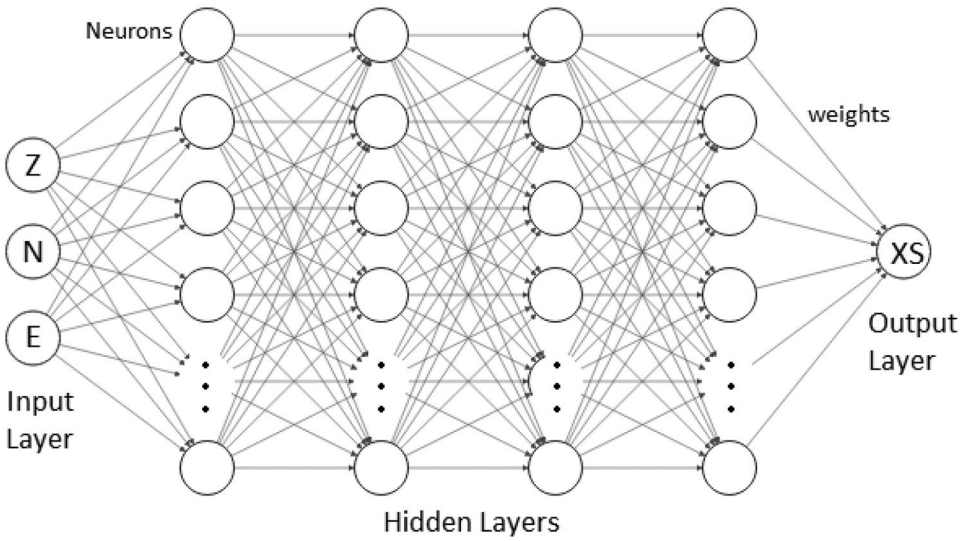

Fig. 1 ANN with (50-50-50-20) structure for the prediction of photo-neutron cross-sections for p-shell stable target nuclei

shown the (50-50-50-20) NN structure which is one of the used structures in this study for the determinations of the reaction cross-sections for p-shell stable nuclei. The other used NN structures have been given in Sect. 3. The inputs were proton number (Z), neutron number (N) of the target nuclei and photon energy (E) impinging upon the target. Only stable or very-long living isotopes have been considered as target nuclei which are ^{7}Li, ^{9}Be, ^{10}Be ($1.51x10^{6}$ years), ^{10}B, ^{11}B, ^{12}C, ^{13}C, ^{14}C (5700 years), ^{14}N, ^{15}N and ^{16}O isotopes. The desired output was photo-neutron reaction cross-section for these different isotopes.

The main goal of the method is the determination of the final weight values between neurons by starting random initial values. The NN with best weights gives the NN outputs as close as to the desired values of the problem. In the training stage, NN is trained for the determination of the final best weights by given input and output data values. By the appropriate modifications of the weights, NN modifies its weights until an acceptable error level between NN and desired outputs. The error function was mean square error (MSE) in this study. In the test stage, another dataset of the problem is given to NN and the results are predicted by using the final weights obtained in the training process. If the predictions of the test data are well, the ANN is considered to have learned the relationship between input and output data.

In this work, Python programming language for the neural network calculations wasused. Python programming language contains fast and practical libraries such as *pandas, numpy, keras*, etc. The data for (γ, n) reaction cross-sections in the literature are studied from threshold energy values to 200 MeV. Total of 537 cross-section data has been used for the calculations for p-shell nuclei. The whole data were obtained from TENDL reaction cross-section database [6]. All data was divided into two separate sets for training (80%) and test (20%) stages in the calculations. This separation was made randomly according to the energies, regardless of the separation of nuclei. Therefore, in both training and test sets, cross-section data of each isotope is available at different energies. For each nucleus, between 30 and 40 datapoints in the training dataset and between 8 and 10 datapoints in the test dataset were available corresponding to different energy values. Although cross-section values above 100 MeV are very close to zero, we did not set an upper limit on the energy we obtained from the literature in order to make the training comprehensive and to perform machine learning in a wider data range. The deep sequentialneural network model consisting of sequential layers has been used. Each layer added to the deep network is fully connected. In the training stage of NN, the *adam* optimization algorithm [20], which is often preferred in deep learning studies, has been used for optimization.

3 Results and Discussion

Although there are experimental cross-section data available in the literature [7], the data do not cover all energy values for target materials. Besides, it is important to have cross-section information for each desired energy value of the photons to be sent on the target materials. Neural network (NN) methods are a suitable and easy way for this task. In the calculations of the present study, NN method has been employed for the determination of cross-sections whose inputs are atomic number (Z), neutron number (N) of the target material and energy (E) of the incoming photons. Different numbers of hidden layer and neuron have been used which gives the optimal results for their hidden layer configuration classes. These are one hidden layer with 20 neurons, three hidden layers with (3-8-8) configuration, three hidden layers with (50-20-10) configuration, four hidden layers with (50-50-20-20), four hidden layers with (50-50-50-20) and five hidden layers with (50-50-20-20-10) configuration, respectively. Apart from these, although we tried many different configurations, we presented the ones that gave the best results in our study. Our hierarchical choices in the NN topology are to clearly demonstrate the effect of the numbers of the hidden layer and the hidden neurons on the results. That is to say, we have got preferable results from 20 neurons for the one hidden layer structure than the other neuron number structures for one hidden layer. For each structure, we have used both ReLU and tanh activation functions separately for the comparison of the results.

After the determination of the final weights in the training, the NN has been first used on the training datasets. According to the results of NN with ReLu, the best estimation on the training dataset has been obtained for (50-50-50-20) structure with the MSE (minimum square error) and MAE (mean absolute error) values of 0.021 mb and 0.082 mb. The maximum deviations (MD) from literature data for this NN structure are 0.734 mb for ^{10}Be at 20 MeV photon energy. In the calculations, tanh activation function has also been used. The corresponding MSE, MAE and MD values on the training dataset for tanh activation function are 0.025 mb, 0.075 mb and 0.867 mb. The MD has been observed for ^{14}C at 19 MeV photon energy. The MSE value from ReLU activation function is slightly better than the tanh results on the training dataset. The estimations of other NN structures have been shown in Table 1. For ReLU function, the MD have been observed between 1.510 and 9.912 mb for ^{13}C at 18 MeV, ^{9}Be at 19 MeV, ^{10}Be at 19 MeV, ^{9}Be at 24 MeV and ^{9}Be at 17 MeV for the NN structure of (20), (3-8-8), (50-20-10), (50-50-20-20) and (50-50-20-20-10). For tanh function, the MD have been observed between 1.336 and 9.248mb for ^{10}Be at 20 MeV,

Table 1 Different structure neural network results for the estimations of cross-sections (units in mb)

		Training			*Test*		
Hidden neuron number	**Activation function**	**MSE**	**MAE**	**MD**	**MSE**	**MAE**	**MD**
20	ReLU	4.473	1.182	9.771	3.555	1.115	7.227
3-8-8	ReLU	4.767	1.095	9.912	7.563	1.404	9.984
50-20-10	ReLU	0.840	0.385	6.107	1.099	0.497	5.925
50-50-20-20	ReLU	0.123	0.141	2.689	2.377	0.558	7.481
50-50-50-20	ReLU	0.021	0.082	0.734	0.093	0.103	1.654
50-50-20-20-10	ReLU	0.040	0.109	1.510	1.078	0.391	7.504
20	tanh	2.688	0.737	9.248	6.005	1.256	9.973
3-8-8	tanh	3.099	0.861	9.037	3.830	0.945	9.530
50-20-10	tanh	0.140	0.158	3.631	0.260	0.269	2.003
50-50-20-20	tanh	0.116	0.169	2.366	0.656	0.332	6.313
50-50-50-20	tanh	0.025	0.075	0.867	0.258	0.177	3.271
50-50-20-20-10	tanh	0.038	0.093	1.336	0.325	0.234	3.174

^{11}B at 18 MeV, ^{14}C at 17 MeV, ^{14}C at 15 MeV and ^{10}Be at 20 MeV for the NN structure of (20), (3-8-8), (50-20-10), (50-50-20-20) and (50-50-20-20-10), respectively.

For the seeing of the generalization capability of constructed NN, it has been tested on the test datasets. According to the results, the best predictions on the test dataset have been obtained for the same NN structure (with ReLu) with the MSE and MAE values of 0.093 mb and 0.103 mb. The MD from literature data for this NN structure is 1.654 mb for ^{15}N at 22 MeV photon energy. The corresponding MSE, MAE and MD values on the training dataset for tanh activation function are 0.258 mb, 0.177 mb and 3.271 mb. The MD has been observed for ^{13}C at 15 MeV photon energy. The MSE value from ReLU activation function is about 2.8 factors better than the tanh results on the test dataset. The predictions of other NN structures have also been shown in Table 1. For the ReLU function, the MD have been observed between 5.925 and 9.984 mb for ^{14}C at 26 MeV, ^{15}N at 16 MeV, ^{14}C at 19 MeV, ^{10}Be at 22 MeV and ^{14}C at 17 MeV for the NN structure of (20), (3-8-8), (50-20-10), (50-50-20-20) and (50-50-20-20-10). For tanh function, MD have been observed between 2.003 and 9.973mb for ^{9}Be at 20 MeV, ^{7}Li at 22 MeV, ^{14}N at 16 MeV, ^{14}C at 18 MeV and ^{9}Be at 22 MeV for the NN structure of (20), (3-8-8), (50-20-10), (50-50-20-20) and (50-50-20-20-10).

In Fig. 2, we have given the best NN predictions of (50-50-50-20) structure with ReLU activation function on the training dataset in comparison with the available literature data. Although the data is highly non-linear, ANN estimations are in harmony with the literature data. The peaks belong to ^{7}Li, ^{9}Be, ^{10}Be, ^{10}B, ^{11}B, ^{12}C, ^{13}C, ^{14}C, ^{14}N, ^{15}N and ^{16}O isotopes. The largest cross-section has been obtained for ^{14}C isotopes with its maximum value of 33.5 mb at 17 MeV energy value. Its literature value is 33.1 mb. The smallest cross-section has been seen for ^{12}C isotopes. The maximum

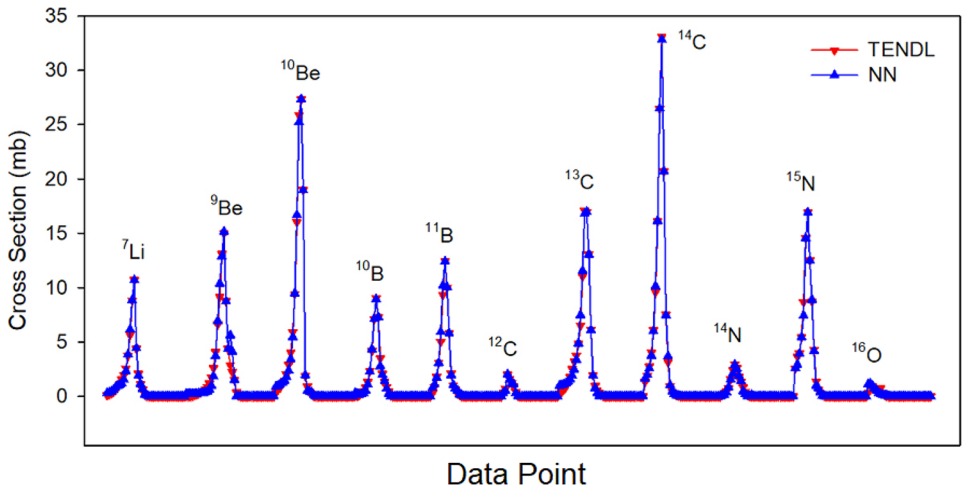

Fig. 2 Literature (TENDL) data and best NN estimations with (50-50-50-20) structure on photo-neutron reaction cross-section on stable p-shell nuclei (top) and differences between them (bottom)

of the cross-section for this isotope is 2.03 mb at 22 MeV whereas the literature value is 2.00 mb.

The maximum cross-section values are 10.23 mb at 22 MeV for ^{7}Li, 14.66 mb at 20 MeV for ^{9}Be, 26.70 mb at 19 MeV for ^{10}Be, 9.00 mb at 19 MeV for ^{10}B, 12.33 mb at 18 MeV for ^{11}B, 2.03 mb at 22 MeV for ^{12}C, 17.17 mb at 18 MeV for ^{13}C, 33.45 mb at 17 MeV for ^{14}C, 3.28 mb at 17 MeV for ^{14}N, 16.96 mb at 17 MeV for ^{15}N and 0.96 mb at 17 MeV for ^{16}O. Whereas the literature values are 10.72, 14.99, 27.33, 9.05, 12.47, 2.00, 16.95, 33.10, 2.96, 16.93 and 0.96, respectively. The cross-sections get their maximums for the nuclei between 17-22 MeV in the investigated energy range from threshold energies to 200 MeV. The reaction thresholds are 8, 2, 7, 9, 12, 19, 5, 9, 11, 11 and 16 MeV for ^{7}Li, ^{9}Be, ^{10}Be, ^{10}B, ^{11}B, ^{12}C, ^{13}C, ^{14}C, ^{14}N, ^{15}N and ^{16}O isotopes, respectively.

In Figs. 3, 4, 5, 6 and 7, we have given the differences between the NN predictions and the TENDLvalues on relevant cross-section data. These have been shown for both training and test datasets separately for either ReLU or tanh activation functions.

For the 20 neurons in one hidden layer NN structure, the estimations on the training data for tanh activation function are better than the ReLU results. Namely, the training of the NN has been performed better for tanh, whereas the test of the NN is worst (Fig. 3). However, it is not appropriate to use this NN structure since the estimates are spread around 10 mb. For the (3-8-8) hidden layer configuration of NN, tanh activation function gives better results on both train and test datasets (Fig. 4). But since the estimates still reach around 10 mb, this structure is also not suitable for use.

For the (50-20-10) hidden layer configuration of NN which is larger in terms of neuron numbers, the estimations for tanh activation function are better than the ReLU results. The results are 6 and 4 factors better for train and test datasets, respectively (Fig. 5). The deviations for predictions on test datasets are between -2 and 2 mb indicate that the larger structures become convenient for the problem. For the (50-50-20-20) hidden layer configuration of NN, the estimations for tanh activation function are slightly better than the ReLU results on the training dataset. Furthermore, the predictions on the test datasets with tanh function are 3.6 factors better (Fig. 6). Still, the NN structure should be improved for the good estimations on the cross-section data, especially for ReLU.

For the (50-50-50-20) hidden layer configuration of NN, the estimations for ReLU activation function are somewhat better than the tanh results on both train and test datasets (Fig. 7). It is clear in the figure that the predictions are concentrated between -1 and 1 mb. In the calculations carried out within the scope of this study, the (γ, n) reaction cross-sections of the p-shell nuclei were obtained with the highest accuracy in this NN structure.

Lastly, we have tried to larger the hidden layer number structure with the (50-50-20-20-10) configuration. For this NN, the training has been performed better by using tanh activation function than ReLu. The estimations on the training dataset are 1.7 factors better than the estimations by using ReLu. For the predictions on the test

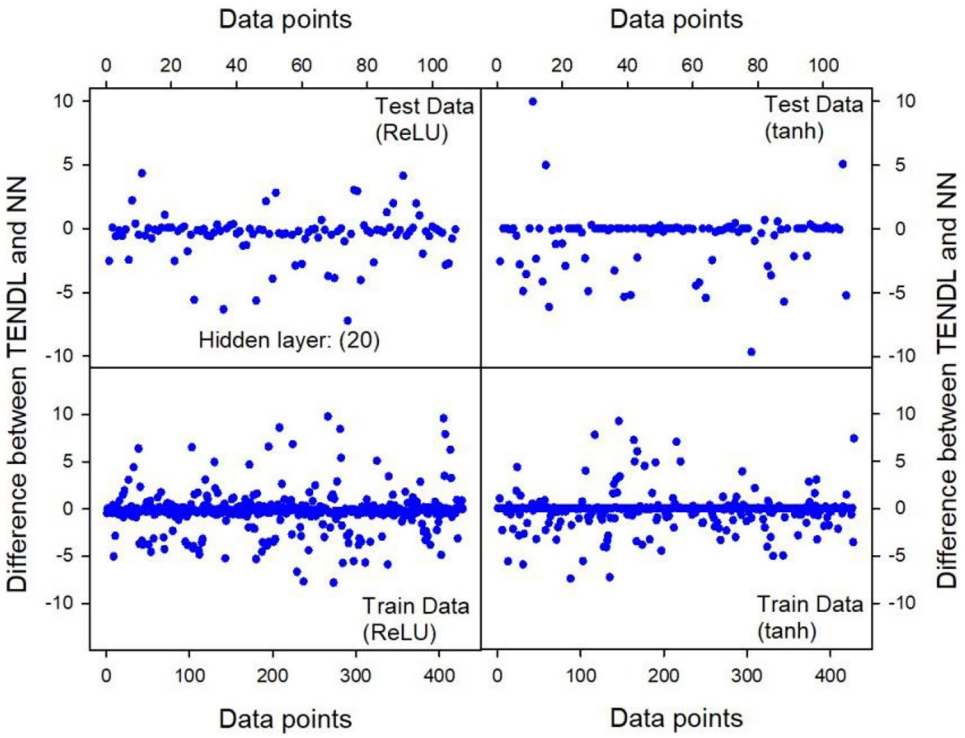

Fig. 3 Difference between literature (TENDL) data and NN (20) estimations on the test (top) and train(bottom) datasets with ReLU (left) and tanh (right) functions

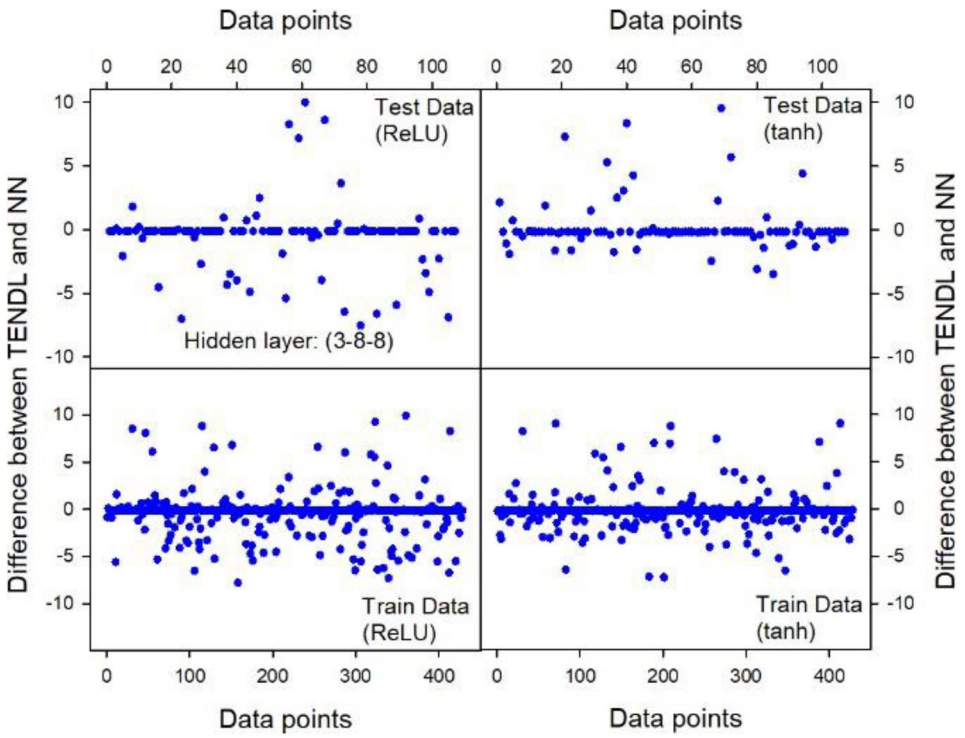

Fig. 4 Difference between literature (TENDL) data and NN (3-8-8) estimations on the test (top) and train (bottom) datasets with ReLU (left) and tanh (right) functions

dataset, tanh gives 3.3 factors better results than those of ReLU (Fig. 8). The fact that the MSE values obtained here were larger than the previous NN configuration showed that using more than four hidden layers again worsened the results.

In the previous part of the study, the theoretical model results obtained from the TENDL database were used in machine learning, and the results produced by NN were emphasized. For this purpose, the data obtained as a result of the NN training were compared with the

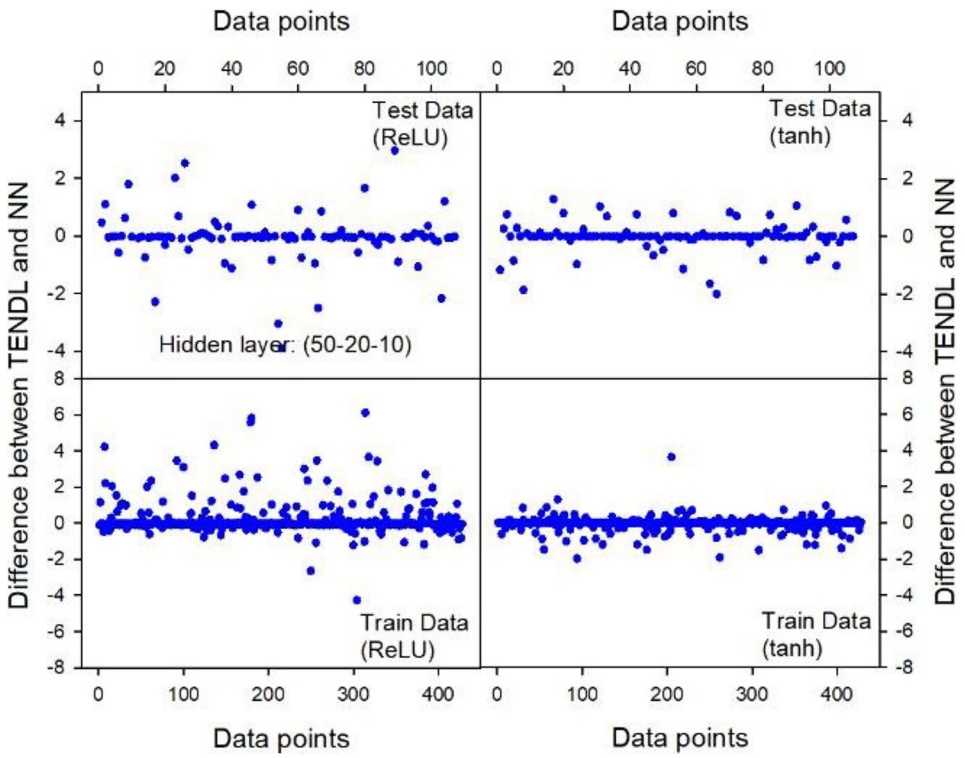

Fig. 5 Difference between literature (TENDL) data and NN (50-20-10) estimations on the test (top) and train (bottom) datasets with ReLU (left) and tanh (right) functions

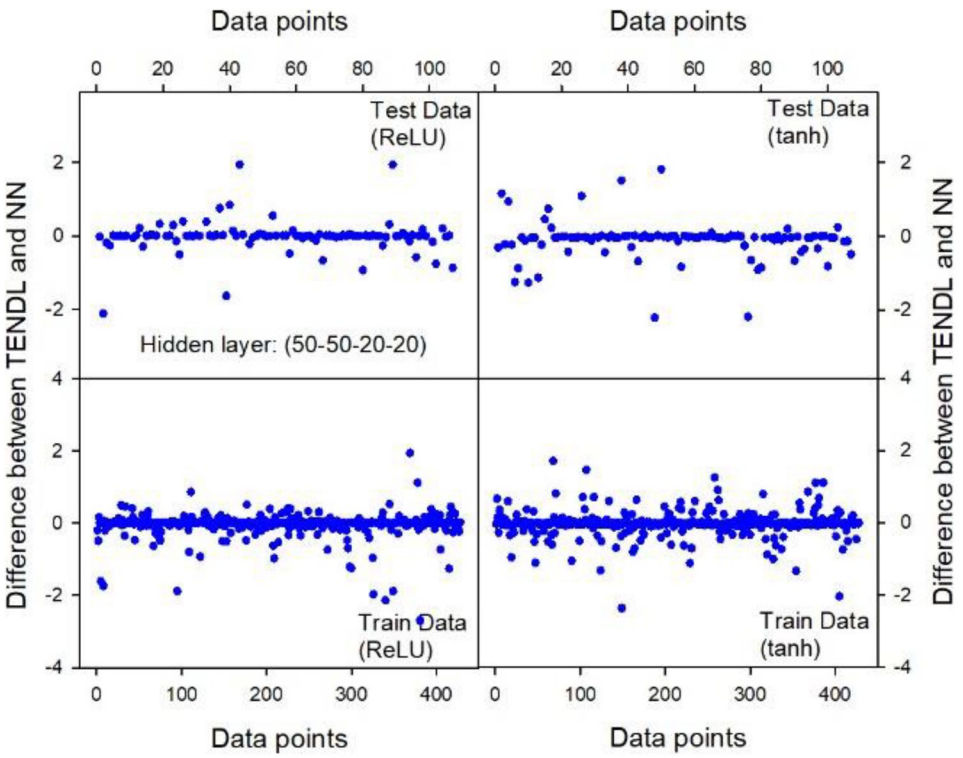

Fig. 6 Difference between literature (TENDL) data and NN (50-50-20-20) estimations on test (top) and train (bottom) datasets with ReLU (left) and tanh (right) functions

TENDL data on the training and test data sets and how well the training was performed was examined. The effects of the number of hidden layers and the number of hidden neurons on the success of the training were investigated, and the results were presented separately. After this stage of the study, it was analyzed whether any improvement, albeit a small one, was made on the theoretical model results. For this purpose, about

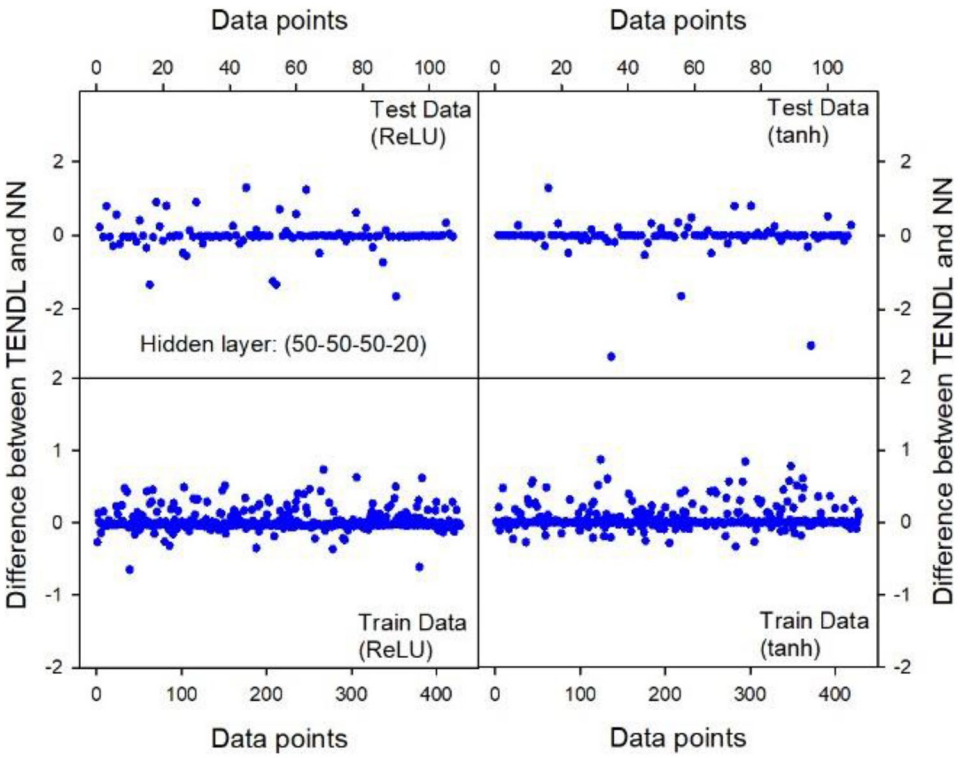

Fig. 7 Difference between literature (TENDL) data and NN (50-50-50-20) estimations on the test (top) and train (bottom) datasets with ReLU (left) and tanh (right) functions

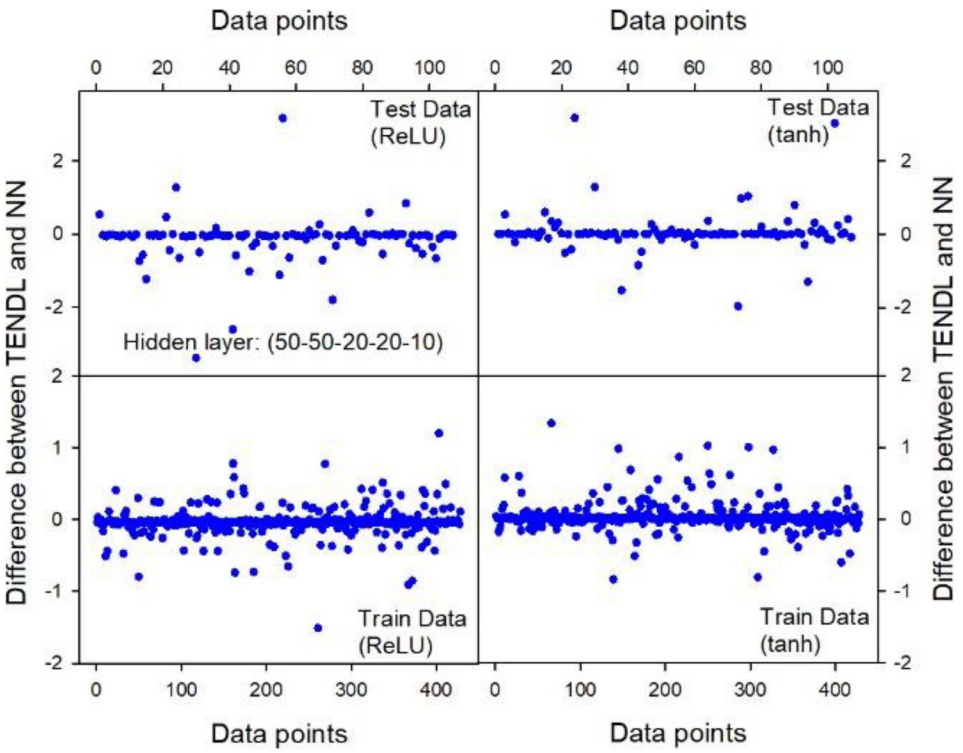

Fig. 8 Difference between literature (TENDL) data and NN (50-50-20-20-10) estimations on the test (top) and train (bottom) datasets with ReLU (left) and tanh (right) functions

50 experimental (γ, n) reaction cross-section data [7] available in the literature for p-shell nuclei are listed. Among these, 26 of them, which are compatible with the reactions and energies we used in the study, are listed in Table 2. Our criterion when comparing the closest energy was to choose the experimental energy value as close as possible to the energy value in our theoretical dataset. As can be seen from the table, the experimental energy value (E_{exp}) compared with the theoretical energy value (E) is close to each other. Of course, it is obvious that even very small differences will create sudden large changes in the cross-section. However, since we made the comparison on both the TENDL data and the NN results simultaneously, it was ignored that this could have a major impact on the analysis.

We performed this comparison with the NN results in the configuration (50-50-50-20) where the best results were obtained. As can be seen from the table, this comparison includes one data each for Li and Be, 4 data for B, 14 data for C, 2 data for N and 4 data for O. The experimental (γ, n) reaction cross-section ($\boldsymbol{\sigma_{exp}}$) and the corresponding energy (E_{exp}) available in the literature were compared with the cross-sections corresponding to the theoretical energy values (E). As mentioned earlier, the closest energies were compared with each other. For example, for ^{7}Li, there is information about the cross-section of this reaction corresponding to 14.75 MeV in the literature. We made the comparison in our study over the cross-section corresponding to the energy value of 15 MeV. Besides, in case of many experimental data close to the theoretical energy, we preferred the value closest in energy. For example, in comparison with the theoretical cross-section at 24 MeV for ^{16}O nuclei, we used the experimental cross-section value corresponding to 24.05 MeV in the literature. However, cross-section data for this isotope were also available at energies of 24.1, 24.22 and 24.202 MeV.

In the table, the absolute values of the deviations of the experimental and theoretical results of the reactions considered are given separately for TENDL, NN (with ReLu) and NN (with tanh). As a result of examining the results one by one, it was seen that the deviation between the NN results and the experimental data was generally less than the deviations of the bare TENDL values from the experimental. This shows that NN provides a slight (~2%) improvement over the theoretical data. The MSE and MAE values for the deviations of the TENDL data from the experimental data are 36.400 mb and 4.919 mb, respectively. However, the MSE values for NN (with ReLu) and NN (with tanh) are 36.128 mb and 36.170 mb, and the MAE values are 4.783 mb and 4.874 mb. It is seen that these error indicator values are lower than the bare TENDL values. Taking an overview of the table, the presence of large deviations from a few values led to high values in MSE and MAE values.

Table 2 Comparison of existing experimental data and TENDL data and the NN results in the structure (50-50-50-20) produced by using them

						NN (50-50-50-20)		Absolute Deviation		
Z	**N**	**E_{exp} (MeV)**	**σ_{exp} (mb)**	**E (MeV)**	**σ_{TENDL}**	**σ_{ReLu}**	**σ_{tanh}**	**σ_{TENDL}**	**σ_{ReLu}**	**σ_{tanh}**
3	4	14.75	0.932	15	1.548	1.185	1.532	0.616	0.253	0.600
4	5	21.207	2.96	22	8.774	8.154	5.600	5.814	5.194	2.640
5	5	22.001	5.55	22	3.506	3.511	3.136	2.044	2.039	2.414
5	6	19.491	3.99	19	10.031	10.09	9.619	6.041	6.100	5.629
5	6	21.503	3.66	22	2.099	2.188	2.699	1.561	1.472	0.961
5	6	26.58	3.79	26	0.591	0.922	0.789	3.199	2.868	3.001
6	6	21	3.3	19	0.301	1.638	1.822	2.999	1.662	1.478
6	6	22	8.1	22	1.998	1.588	0.976	6.102	6.512	7.124
6	6	23.5	11.5	24	1.596	1.371	0.798	9.904	10.129	10.702
6	6	25.6	5.9	26	1.229	0.984	0.595	4.671	4.916	5.305
6	6	30.069	3.56	30	0.420	0.564	0.322	3.140	2.996	3.238
6	7	13.817	3.94	14	4.877	4.342	4.336	0.937	0.402	0.396
6	7	15.07	1.93	15	6.529	6.350	6.622	4.599	4.420	4.692
6	7	20.58	4.25	19	13.071	12.901	12.092	8.821	8.651	7.842
6	7	20.58	4.25	20	6.156	6.154	5.896	1.906	1.904	1.646
6	7	20.976	6.6	22	1.963	1.662	1.099	4.637	4.938	5.501
6	7	23.77	8.11	24	0.962	0.851	0.386	7.148	7.259	7.724
6	8	15.417	8.956	15	16.087	16.824	15.483	7.131	7.868	6.527
6	8	22.493	5.267	22	0.942	1.379	1.161	4.325	3.888	4.106
6	8	28.892	3.779	28	0.102	0.129	0.223	3.677	3.650	3.556
7	7	23.343	14.65	24	0.416	0.639	0.592	14.234	14.011	14.058
7	8	22.964	11.68	22	1.363	1.556	1.0796	10.317	10.124	10.600
8	8	17.301	1.85	17	0.960	2.076	1.239	0.890	0.226	0.611
8	8	19.646	1.6	20	0.601	1.181	0.583	0.999	0.419	1.017
8	8	22.107	10.514	22	0.745	0.774	0.570	9.769	9.740	9.944
8	8	24.05	8.1	24	0.760	0.600	0.548	7.340	7.500	7.552
							MAE	4.919	4.783	4.874
							RMSE	36.400	36.128	36.170

4 Conclusions

In this work, (γ, n) photo-neutron reaction cross-sections for the stable or long-lived isotopes in p-shell have been predicted by using neural network (NN) methods with the different hidden layer and neuron combinations in the threshold to 200 MeV energy range. The results have been compared with each other and the available literature data. According to the results, we have seen that from our implementations, on the shallow NN models, tanh activation function is better than ReLU. However, as our models become deeper, the accuracy difference between tanh and relu have been rather decreased. In this context, we think that the crucial hyperparameters are the size of hidden layer and neuron numbers of each layers. Therefore, one can use the NN methods for the obtaining of photo-neutron reaction cross-sections whose values are not available in the literature. In detail, the obtained better results have generally come from the activation function of tanh. But the present problem, (50-50-50-20) hidden layer configuration in four hidden layers with ReLU function has given the best results. At the end of the study, we saw that the machine learning results obtained using from the theoretical models were closer to the experimental data. This indicates that the NN method generalizes by understanding the relationship between the data. Thus, we conclude that any theoretical model results can be improved somewhat with the support of machine learning.

Funding This work is supported by the Scientific Research Project Fund of Sivas Cumhuriyet University under the project number F-2022-667.

Declarations

Conflict of Interest The authors declared that they have no conflict of interest.

References

1. K. Strauch, Recent Studies of Photonuclear Reactions. Annu. Rev. Nucl. Sci. **2**, 105 (1953). https://doi.org/10.1146/annurev.ns.02.120153.000541
2. J. Chadwick, M. Goldhaber, A Nuclear Photo-effect: Disintegration of the Diplon by -Rays. Nature **134**, 237 (1934). https://doi.org/10.1038/134237a0
3. S. Akkoyun, T. Bayram, F. Dulger et al., Energy level and half-life determinations from photonuclear reaction on Ga target. Int. J. Mod. Phys. E **25**, 1650045 (2016). https://doi.org/10.1142/S0218301316500452
4. B.S. Ishkhanov, V.N. Orlin, Description of cross sections for photonuclear reactions in the energy range between 7 and 140 MeV. Phys. At. Nucl. **72**, 410 (2009). https://doi.org/10.1134/S1063778809030041
5. Y. Utsuno, N. Shimizu, T. Otsuka et al., Photonuclear reactions of calcium isotopes calculated with the nuclear shell model. Prog. Nucl. Energy **82**, 102 (2015). https://doi.org/10.1016/j.pnucene.2014.07.036
6. A.J. Koning, D. Rochman, J.-Ch. Sublet et al., TENDL: Complete Nuclear Data Library for Innovative Nuclear Science and Technology. Nucl. Data Sheets **155**, 1 (2019). https://doi.org/10.1016/j.nds.2019.01.002
7. International Atomic Energy Agency, *Handbook on Photonuclear Data for Applications Cross-sections and Spectra, IAEA-TECDOC-1178* (IAEA, Vienna, 2000)
8. T. Bayram, S. Akkoyun, S.O. Kara, A study on ground-state energies of nuclei by using neural networks. Ann. Nucl. Energy **63**, 172 (2014). https://doi.org/10.1016/j.anucene.2013.07.039
9. S. Akkoyun, Estimation of fusion reaction cross-sections by artificial neural networks. Nucl. Instrum. Methods Phys. Res. Sect. B Beam Interact. Mater. At. **462**, 51 (2020). https://doi.org/10.1016/j.nimb.2019.11.014
10. S. Akkoyun, T. Bayram, S.O. Kara, et al., An artificial neural network application on nuclear charge radii. J. Phys. G Nucl. Part. Phys. **40**, 055106 (2013). https://doi.org/10.1088/0954-3899/40/5/055106
11. S. Akkoyun, T. Bayram, ve T. Turker, Estimations of beta-decay energies through the nuclidic chart by using neural network. Radiat. Phys. Chem. **96**, 186 (2014). https://doi.org/10.1016/j.radphyschem.2013.10.002
12. S. Akkoyun, S.O. Kara, An approximation to the cross sections of Zlboson production at CLIC by using neural networks. Cent. Eur. J. Phys. **11**, 345(2013). https://doi.org/10.2478/s11534-012-0168-y.
13. S.O. Kara, S. Akkoyun, T. Bayram, Probing for leptophilic gauge boson Zl at ILC with $\sqrt{s} = 1$ TeV by using ANN. Int. J. Mod. Phys. A **29**, 1450171 (2014). https://doi.org/10.1142/S0217751X14501711
14. N. Yildiz, S. Akkoyun, K.A. Hüseyin, Consistent Empirical Physical Formula Construction for Gamma Ray Angular Distribution Coefficients by Layered Feedforward Neural Network. Cumhur. Sci. J. **39**, 928 (2018). https://doi.org/10.17776/csj.476733
15. T.U. Bayram, S.E. Akkoyun, Ş. Şentürk, Adjustment of Non-linear Interaction Parameters for Relativistic Mean Field Approach by Using Artificial Neural Networks. Phys. At. Nucl. **81**, 288 (2018). https://doi.org/10.1134/S1063778818030043
16. S. Akkoyun, Time-of-flight discrimination between gamma-rays and neutrons by using artificial neural networks. Ann. Nucl. Energy **55**, 297 (2013). https://doi.org/10.1016/j.anucene.2013.01.006
17. N. Yildiz ve S. Akkoyun, Neural network consistent empirical physical formula construction for neutron–gamma discrimination in gamma ray tracking. Ann. Nucl. Energy **51**, 10 (2013). https://doi.org/10.1016/j.anucene.2012.07.042
18. S. Akkoyun, T. Bayram, N. Yildiz, Estimations of Radiation Yields for Electrons in Various Absorbing Materials. Cumhur. Üniversitesi Fen-Edeb. Fakültesi Fen Bilim. Derg. **37**, 59 (2016)
19. S. Haykin, *Neural Networks: A Comprehensive Foundation*, 2nd edn. (Prentice Hall, Upper Saddle River, N.J, 1998)
20. D. P. Kingma ve J. Ba, Adam: A Method for Stochastic Optimization. arXiv14126980 Cs (2017)